SANDIA REPORT
SAND2007-6487
Unlimited Release
Printed October 2007

The Role of Z-Pinch Fusion Transmutation of Waste in the Nuclear Fuel Cycle

Benjamin B. Cipiti, William J. Martin, Thomas A. Mehlhorn, Gary E. Rochau, James D. Smith, Ryan Grady, Phiphat Phruksarojanakun, Paul P.H. Wilson, Avery Guild-Bingham, Pavel Tsvetkov, Thomas E. Drennen, William Kamery

Prepared by
Sandia National Laboratories
Albuquerque, New Mexico 87185 and Livermore, California 94550

Sandia is a multiprogram laboratory operated by Sandia Corporation,
a Lockheed Martin Company, for the United States Department of Energy's
National Nuclear Security Administration under Contract DE-AC04-94AL85000.

Issued by Sandia National Laboratories, operated for the United States Department of Energy by Sandia Corporation.

Available to DOE and DOE contractors from
U.S. Department of Energy
Office of Scientific and Technical Information
P.O. Box 62
Oak Ridge, TN 37831

Telephone: (865)576-8401
Facsimile: (865)576-5728
E-Mail: reports@adonis.osti.gov
Online ordering: http://www.osti.gov/bridge

Available to the public from
U.S. Department of Commerce
National Technical Information Service
5285 Port Royal Rd
Springfield, VA 22161

Telephone: (800)553-6847
Facsimile: (703)605-6900
E-Mail: orders@ntis.fedworld.gov
Online order: http://www.ntis.gov/help/ordermethods.asp?loc=7-4-0#online

SAND2007-6487
Unlimited Release
Printed October 2007

The Role of Z-Pinch Fusion Transmutation of Waste in the Nuclear Fuel Cycle

B.B. Cipiti[1], W. J. Martin[1], T.A. Mehlhorn[1], G.E. Rochau[1], J.D. Smith[1], R. Grady[2], P. Phruksarojanakun[2], P.P.H. Wilson[2], A. Guild-Bingham[3], P. Tsvetkov[3], T.E. Drennen[4], W. Kamery[4]

[1]Sandia National Laboratories, P.O. Box 5800, Albuquerque, NM 87185-0748
[2]University of Wisconsin, 1500 Engineering Dr, Madison, WI 53706
[3]Texas A&M University, 129 Zachry Engineering Center, College Station, TX 77843-3133
[4]Hobart & William Smith College, 300 Pultney St, Geneva, NY 14456

Abstract

The resurgence of interest in reprocessing in the United States with the Global Nuclear Energy Partnership has led to a renewed look at technologies for transmuting nuclear waste. Sandia National Laboratories has been investigating the use of a Z-Pinch fusion driver to burn actinide waste in a sub-critical reactor. The baseline design has been modified to solve some of the engineering issues that were identified in the first year of work, including neutron damage and fuel heating. An on-line control feature was added to the reactor to maintain a constant neutron multiplication with time. The transmutation modeling effort has been optimized to produce more accurate results. In addition, more attention was focused on the integration of this burner option within the fuel cycle including an investigation of overall costs. This report presents the updated reactor design, which is able to burn 1320 kg of actinides per year while producing 3,000 MWth.

Acknowledgement

The authors would like to acknowledge the support of Laboratory Directed Research and Development Project 81753 under the guidance of Tom Mehlhorn and Dan Sinars, and past work as part of the Z-IFE Project under the guidance of Craig Olson and Gary Rochau for this research.

Contents

Figures

Tables

Executive Summary

The Z-Pinch fusion technology developed at Sandia National Laboratories has been examined for potential alternative uses. High energy neutrons produced from fusion are useful for transmuting nuclear waste into more benign materials. With increasing concerns about the buildup of spent nuclear fuel in the United States, the design of a Z-Pinch-driven waste burner was initiated. This report discusses the baseline design for such a waste burner with attention to transmutation potential, engineering issues, and economics.

The "In-Zinerator" design uses a Z-Pinch fusion source to generate neutron pulses once every ten seconds to drive a sub-critical actinide blanket. Transuranic actinides from spent nuclear fuel (including Np, Pu, Am, and Cm) are contained in a molten salt fuel, $(LiF)_{0.85}(AnF_3)_{0.15}$. This fuel is contained in tubes which surround the fusion target chamber in an annular array. The Z-Pinch chamber is separated from the actinide blanket by a first wall, and a molten lead coolant is used to remove the heat generated by the actinide tubes. The baseline design assumes 200 MJ fusion targets, fired once every ten seconds, which produce 3000 MW of thermal energy in the actinide blanket.

The geometry has been designed to keep the neutron damage of the reactor components below acceptable levels. Both the first wall and the actinide tubes will receive a neutron dose less than 50 displacements per atom (dpa) after 40 full-power years. The temperature rise within the actinide tubes peaks at 152 ºC after each fusion pulse, and the temperature of the actinide fuel stabilizes at 3225 ºC. Although these two values are still too high for safe operation, minor changes should be able to reduce these values in future work.

A unique aerosol protection scheme has been designed to protect the first wall from x-ray damage. The use of aerosols is possible in the Z-Pinch chamber since the device does not need clean chamber conditions (as compared to laser-driven fusion). About 23.5 kg of tin in an aerosol form per shot was adequate for absorbing the x-rays from the fusion target to prevent damage to the first wall. The aerosol volume fraction was $\alpha = 5.93 \times 10^{-5}$.

A unique aspect of the In-Zinerator is that the continuously recycled fuel leads to changing isotopic ratios with time. In order to keep multiplication constant, the actinide loading within the fuel is gradually increased with time. The actinide loading starts at 15% and needs to be gradually increased to 20% by the end of 40 FPY of operation to maintain a k_{eff} of 0.989. A fine-tuning control mechanism using air leakage rods has been designed which can further adjust the k_{eff} of the system slightly.

At the 3000 MWth power level, the actinide burnup rate equals 1320 kg/yr. It would therefore take 25 In-Zinerators to burn transuranic actinides at the rate that they are produced from the current U.S. light water reactor fleet.

The economics of Z-Pinch waste transmutation have been investigated as well. In an advanced nuclear fuel cycle, reprocessing will likely add 0.3 ¢/kWh to the cost of nuclear energy. Fusion transmutation of waste is competitive with fast reactor transmutation, but both are likely to add an additional 0.5 ¢/kWh to the overall cost of nuclear energy. However, the real question is

whether the dramatic reduction in heat load and radiotoxicity of waste is worth these costs. Advanced fuel cycles can be made more economic if thermal recycling is used first to burn up transuranic actinides as much as possible. Then a smaller number of advanced fusion transmuters or fast reactors could be used to burn up the left over actinides.

There could be several advantages to a fusion-driven waste transmuter. A sub-critical assembly may be more accepted than a critical fast reactor, and it also allows for more versatility in fueling (actinide mixtures with poor fissile content can be burned). A fusion-driven burner can achieve a better support ratio as compared to fast reactors, requiring the building of fewer costly units. Finally, experience in building a fusion driver could pave the way toward a pure fusion energy plant in the future. The current approach of achieving fusion energy through multiple billion-dollar leaps of faith is not working. Intermediate applications like transmutation can offer fusion research the stepping stones it needs.

Acronyms

An	Actinide
DPA	Displacement Per Atom
FP	Fission Product
FPY	Full Power Year
FR	Fast Reactor
GNEP	Global Nuclear Energy Partnership
LWR	Light Water Reactor
MCise	Monte Carlo Inventory Simulation Engine
MCNP	Monte Carlo Neutron Transport (code)
MOX	Mixed Oxide
MT	Metric Ton
RTL	Recyclable Transmission Line
TBR	Tritium Breeding Ratio
TRU	Transuranic Isotopes (Np, Pu, Am, Cm)

The Role of Z-Pinch Fusion Transmutation of Waste in the Nuclear Fuel Cycle

1.0 Introduction

Sandia National Laboratories has been investigating the use of a Z-Pinch fusion reactor as a neutron generator to transmute nuclear waste. The Z-Pinch facility at Sandia uses an intense pulsed power source to generate x-rays which in turn heat a fusion target. The high-energy neutrons liberated from the D-T fusion reaction can be used to induce fission in an actinide-bearing blanket to burn up long-lived actinides.

In the previous year's work, a preliminary design was developed for a Z-Pinch transmutation reactor [1]. This "In-Zinerator" concept was designed to burn 1,280 kg of actinides per year while at the same time producing 1,000 MW_e. The conversion of long-lived actinides to short-lived fission products resulted in a significant decrease in long-term heat load of the waste. A 200 MJ fusion target fired once every ten seconds was found to be adequate to power a sub-critical actinide blanket with a high energy multiplication. The blanket was designed to burn up the transuranic (TRU) isotopes from spent light water reactor (LWR) fuel, including Np, Pu, Am, and Cm.

1.1 Actinide Burning

The current fleet of U.S. LWRs produces on the order of 33.4 metric tons (MT) of TRU per year. The TRU isotopes are responsible for a majority of the long-term decay heat and radiotoxicity of spent nuclear fuel [2,3]. In addition, the TRU contains a great deal of energy that could be further extracted in a reactor. The purpose of transmutation is to both make better use of fissile resources while at the same time dramatically reduce the long-term decay heat and radiotoxicity of waste destined for the repository.

Reactors that can produce fast neutrons have been investigated for TRU destruction since they minimize the buildup of some of the higher order actinides like Cm. However, one of the difficulties of using fast reactors or a fusion-driven actinide burner is that the reactors are complex and immature in commercial development. For this reason, these burners will likely be more expensive than LWRs. It stands to reason that advanced fuel cycles should be examined for ways to minimize the number of these fast systems.

The original In-Zinerator design was able to burn up 1,280 kg of TRU per year while at the same time producing about 3,000 MWth. It would take 26 of these reactors to burn up all of the TRU coming from today's fleet of LWRs. In comparison, the best likely fast reactor (FR) design with a conversion ratio of 0.5 would be able to burn about 156 kg of TRU per year with a 1,000 MW_{th} core. It would then take 213 of these FRs to burn up all of the TRU from today's fleet of LWRs. Section 5 will discuss ways to optimize the fuel cycle to limit the number of burner reactors

required. The economics of Z-Pinch transmutation of waste are examined as compared to other advanced nuclear fuel cycles.

1.2 Engineering Issues Identified in the Previous Year

The 2006 In-Zinerator design was not optimized for the effects of neutron damage and heat removal. Previous results found that the peak neutron damage to the actinide tubes went over 1000 displacements per atom (dpa) by the end of reactor life. For advanced materials, 200 dpa is the limit typically used in fusion reactors and fission reactors before the component needs to be replaced. The current design was modified to address this issue using various geometry changes.

Another problem identified was the intense heating of the actinide mixture after each shot, which was calculated to cause near-instantaneous temperature rises of as much as 700 ºC. This temperature rise is not possible to engineer around due to the formation of shock waves within the tubes. Geometry changes and actinide mixture changes were used to reduce the temperature increase.

A shock mitigation technique was investigated in the previous year, but the idea was examined in more detail for this year's work. A study is presented in this report on shock mitigation of the fusion pulse using an aerosol in the fusion chamber.

Due to changing isotopics within the reactor with time, it was found that control features would be required to maintain a constant multiplication with time. The transmutation modeling has been performed using a University of Wisconsin code, MCise. This model tracks actinide and fission product inventories within the In-Zinerator blanket as a function of time. The modeling was updated to allow for an on-line control capability to keep the fission multiplication constant. Also, some minor errors in the model have been corrected to provide more accurate results.

2.0 New Baseline Design

The parametric studies of the In-Zinerator model in FY06 primarily focused on criticality, tritium breeding, and initial fuel loading of the system. Two major engineering issues were found in the baseline model. First, the radiation damage rate on the first wall peaked at 550 dpa and the radiation damage on the actinide tubes peaked at 1300 dpa after 40 years of operation, both well above the 200 dpa limit. Second, it was estimated that the temperature rise in the fuel tubes due to fission energy multiplication after each pulse was around 700 ºC (much too high). Therefore, the focus on this next design iteration was initiate changes to the system parameters in order to improve upon these engineering constraints.

The average temperature rise in the fuel was reduced by increasing the total fuel mixture volume while decreasing the actinide loading fraction in the fuel. The net effect was to lower the power density of the system, thereby decreasing the maximum energy deposited in the fuel tubes. After further investigation and development of a heat transfer model for the system, the diameter of the fuel tubes was found to be too large for sufficient heat transfer. The poor heat transfer characteristics were primarily due to the low thermal conductivity of LiF, which is believed to approximate the thermal characteristics of the LiF-AnF_3 eutectic fuel mixture [4]. This analysis is discussed in detail in section 2.2, but the key result was that a 2 cm diameter tube would be sufficient for heat removal. The change in fuel tube diameter resulted in a drastic change in the required fuel tube geometry in order for the system to maintain similar neutronics characteristics.

Conveniently, the solution for the average temperature rise issue also helped address the problem associated with the radiation damage to the tubes. To address the radiation damage to the first wall, the distance between the first wall and the fuel region was increased to spread out the neutron damage. The resulting design parameters for the In-Zinerator are presented in Table 1, with all lengths in centimeters. A chamber schematic is shown in Figure 1.

Fuel Tube Pitch	**3.25**
Minimum distance between wall and tubes	**10**
Chamber inner radius	**200**
Chamber outer radius	**205**
Fuel region outer radius	**336.3**
Outer Wall inner radius	**406**
Outer Wall outer radius	**409**
Tube inner radius	**1.0**
Tube outer radius	**1.3**
Li-6 fraction	**0.03**
Chamber height	**600**
AnF fraction	**0.15**
Total Number of tubes	**19182**
Tritium Breeding ratio	**1.35**
keff	**0.989**

Table 1: New In-Zinerator Baseline Design Parameters (all dimensions in cm)

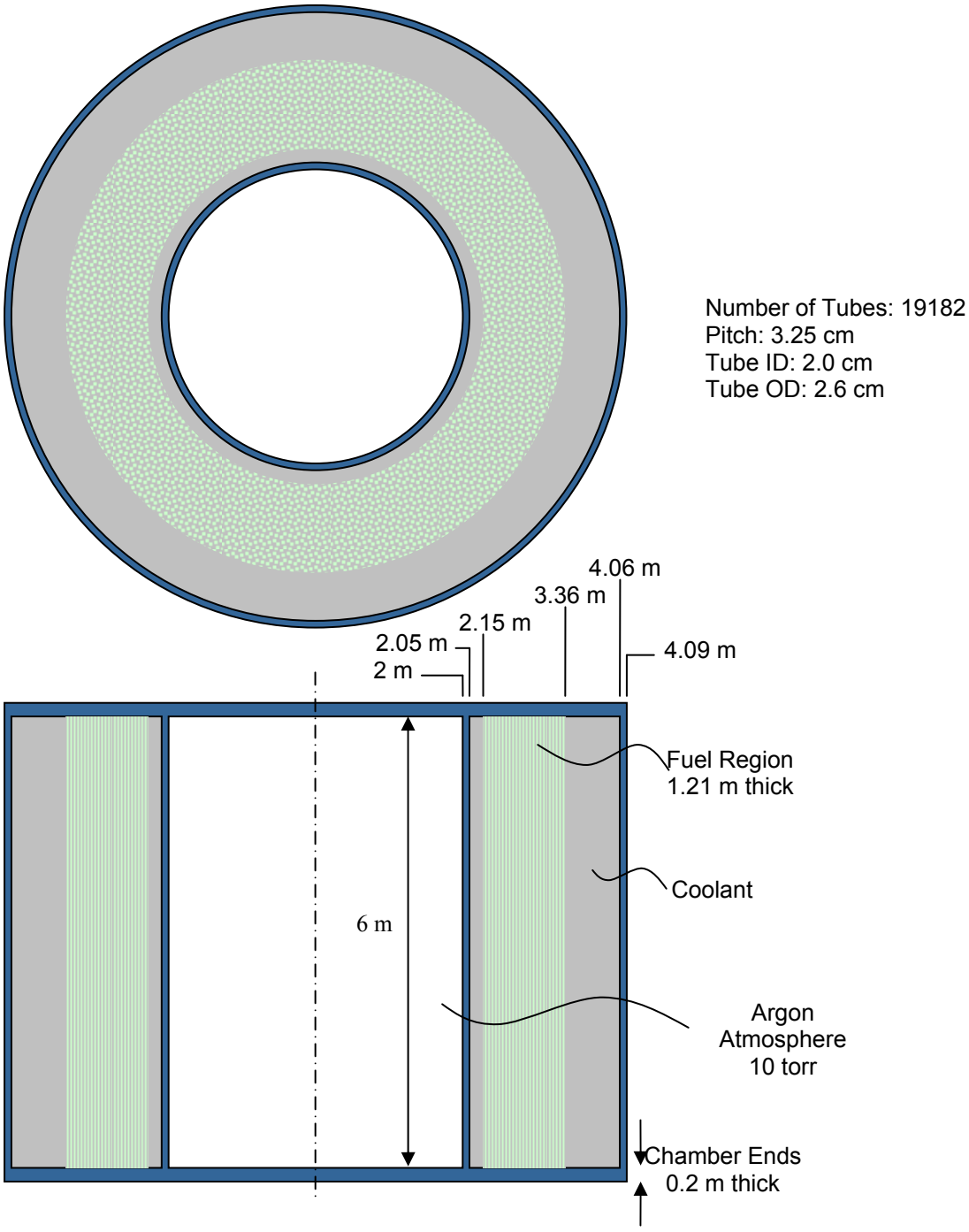

Figure 1: In-Zinerator Design Schematic

The schematic shown in Figure 1 represents the geometry that was modeled in MCNP, so it is somewhat simplistic and does not include components surrounding the reactor vessel. The lead coolant is designed to travel up outside of the actinide tubes and then down toward the outside of

the chamber (thus the large coolant region outside of the tubes). The neutron source efficiency factor was found to be 0.35, which means that only ~1/3 of the fusion neutrons are utilized by the blanket. However, since the fusion component is so small compared to the fission blanket, this does not represent a large loss of neutrons from the system. This loss ultimately is due to the large standoff from the fusion target to the actinide blanket, which is driven by engineering constraints.

The high k_{eff} of 0.989 was required to reach a system neutron multiplication of 30. This value is very close to critical, and could raise safety concerns for a transuranic fuel reactor. Such safety concerns will need to be addressed in future work.

2.1 Neutron Damage Limits

In a fast neutron system, damage due to neutrons is inevitable. Neutron damage to materials is more pronounced for higher energy neutrons. Under fast neutron irradiation, all steels experience radiation-induced hardening and embrittlement. Steels bombarded by fast neutrons also experience swelling (volume increase) and radiation-induced creep. Typically, irradiation causes the hardness and strength to increase with a concurrent decrease in the ductility and toughness due to atom displacements. Highly energetic neutrons can produce collision cascades that may cause multiple atom displacements [5]. A dose of 1 dpa corresponds to stable displacement from their lattice site of all atoms in the material during irradiation near absolute zero, where no recovery due to thermally activated point defect diffusion can occur [6]. A neutron fluence of 10^{21} n/cm^2 in the fusion-fission hybrid system is expected to result in 1 dpa in Hastelloy-N, the structural material that makes up the chamber and fuel tubes.

The first demonstration fusion reactor is expected to have a maximum structural dose of 50–150 dpa at maximum temperatures 550–1000 °C [6]. Previously it was assumed that Hastelloy-N would withstand up to 200 dpa before needing replacement. However, neutron irradiation is accompanied by gas production which further affects mechanical properties. Helium production can occur when isotopes of Fe, Cr, and Ni are present. The helium production rate tends to be higher in Ni rich austenitic steels due to Ni(n, α)Fe reaction. He migration to grain boundaries can lead to embrittlement. Literature has shown that material failure in Hastelloy N may be a risk at 20 dpa due to He embrittlement [7]. It should be noted that other studies have drawn different conclusions based on precipitation, hydrogen generation, and charged-particle irradiations [8]. These studies will not be described in detail here. There is insufficient information to conclude whether helium embrittlement in ferritic/martensitic steels will be the limiting factor in the high energy neutron fusion-fission environment [9].

Analysis of the In-Zinerator model from the previous year demonstrated that radiation damage was much higher than anticipated. The inner chamber was calculated to obtain approximately 550 dpa on the inner chamber wall after 40 full power years (FPY) at an average power of 3000 MW_{th}. This value is much higher than any known material could safely withstand.

An initial study was done to decrease the fluence on the inner chamber wall by adding a coolant region between the inner chamber wall and the fuel tubes. The results showed that simple design changes resulted in reduced radiation damage to structural components. However, a greater reduction of radiation damage would have to be reached to make the In-Zinerator a feasible design. Desired heat transfer and neutronic characteristics were used to establish performance limits. The final result was a design that reduced the maximum dpa experienced by the inner chamber wall to approximately 40 dpa.

More importantly, the modified design also dramatically decreased the dpa experienced by the fuel tubes. Figure 2 shows the radiation damage to the fuel tubes as a function of distance from the center of the chamber. In all cases, the estimated radiation damage was below 50 dpa. Error bars are based on MCNP statistics.

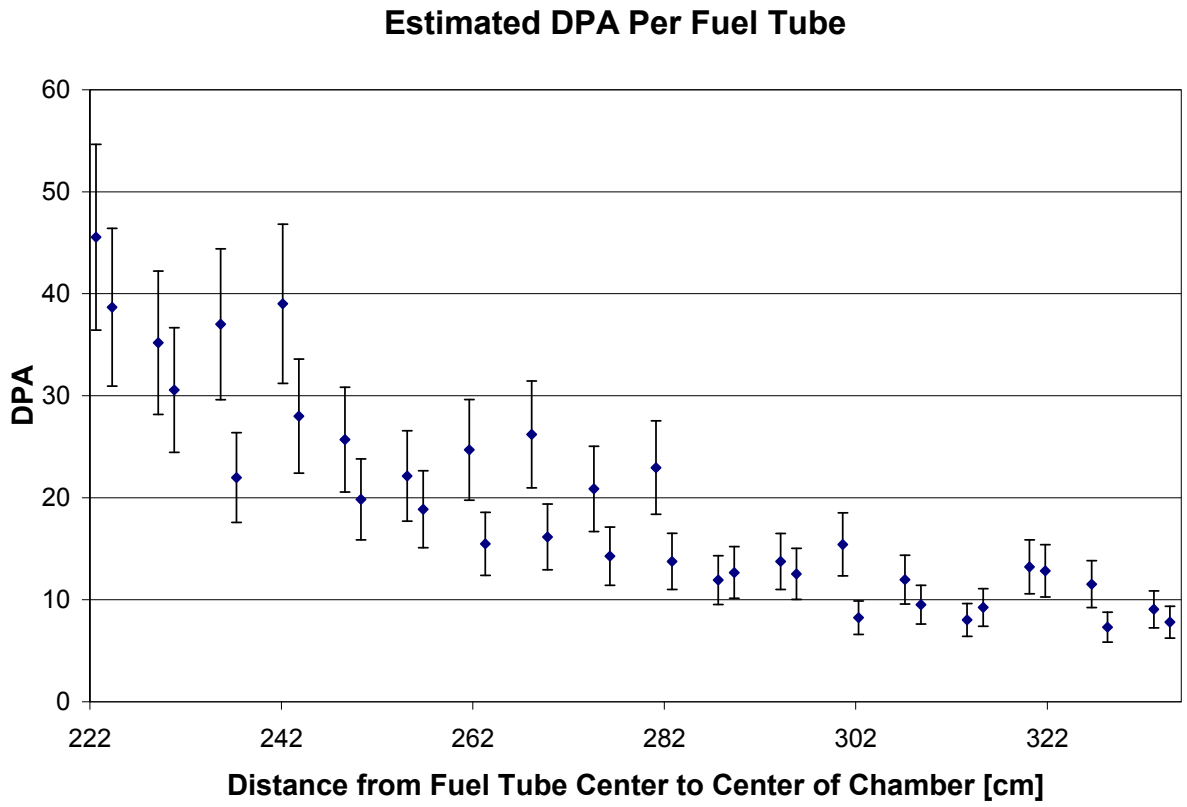

Figure 2: Radiation Damage to the Fuel Tubes

Alternative Reactor Materials

Ferritic/martensitic steel appears to be very resistant to helium embrittlement. For body-centered cubic materials such as ferritic-martensitic steels and the refractory alloys, radiation hardening at low temperatures can lead to a large increase in the ductile to brittle transition temperature. However, it is difficult to find materials that will survive a high thermal and radiation stress environment. F82H is a ferritic/martensitic reduced activation steel which is comprised of

between 8-12 wt% Cr that has been alloyed with low activation elements. F82H is one of the leading candidates for fusion power systems for which a fairly large mechanical and thermal material property database has been developed. Another candidate material is EM10 (Fe-9Cr-Mo) which has been shown to resist swelling up to 200 dpa at temperatures below 500 °C.

Generally, low alloy ferritic materials show an increase in hardness and tensile properties and a decrease in ductility and fracture toughness during high-energy neutron irradiation. Some ferritic/martensitic steels appear to be viable structural materials available for fusion technology. However, most reduced-activation steels are limited to operating temperatures of 550-600°C. If higher operating temperatures are required, new reduced-activation steels will need to be developed. Materials subject to a mechanical load and high temperatures experience thermal creep. Thermal creep rates are also higher in ferritic steels at temperatures above 550°C. Thus, lower operating temperatures may be required.

The corrosion behavior of Pb–Li has been adequately studied for ferritic-martensitic steels and vanadium alloys. The temperature limit of ferritic-martensitic steels due to Pb–Li corrosion is lower than the thermal creep limit of ~450°C due to chemical incompatibility of iron-base alloys with liquid lead. This may be a considerable problem given the coolant choice of lead and fuel choice of the LiF-AnF_3 fuel which is expected to be a liquid at >600°C.

Since the In-Zinerator geometry was changed to limit the radiation damage to all components to below 50 dpa after 40 FPY, Hastelloy-N may still be able to be used as the structural material. The effect of helium embrittlement on structural materials at high temperatures is not well understood, and will require more study in future work.

2.2 Thermal Limits

At the end of the previous year's work, an important conclusion was that the baseline design did not adequately account for thermal limits, and thus led to a fairly unrealistic design. A more accurate thermal analysis was completed this year in order to modify the design.

Thermal Analytic Model Assumptions

The intent of the thermal analytic modeling was to demonstrate the heating of a representative actinide tube due to the fusion neutron pulse and the subsequent cooling of the tube and associated lead coolant. This analysis had several assumptions. Each tube and its associated coolant was assumed to be thermally independent from all other tubes. This model assumed that the liquid actinide mixture in the tube was stationary (or moving slow relative to the pulse repetition rate). The liquid being stationary also implies no mixing or other motion of the fuel liquid. Therefore, no circulation caused by any form of convection was assumed to be present. The sole mode of heat transfer inside the tube was assumed to be conduction. The properties of the liquid fuel were assumed to be constant over the temperature ranges in question since they were general approximations.

There were several other important assumptions with relation to the coolant and cladding material. The lead coolant was assumed to be in the fully-developed turbulent flow regime and heated only through conduction from the tube. It was assumed to enter the model at 675 ºC, move at a constant flow rate, and have a constant density. The cladding material was taken as being thermally thin. The interface was therefore taken as the boundary between the fuel material and coolant, using the inside diameter of the cladding as the boundary's outer diameter.

In order to supply a high enough coolant temperature to the rest of the heat cycle while keeping below the boiling point of lead, a coolant inlet temperature of 675 ºC was assumed. From that temperature, the initial working temperature for the liquid actinide mixture was assumed to be 725 ºC.

The temperature rise produced by each pulse was determined using MCNP. A peaking factor produced in MCNP for the standard tube for this model (2.0 cm OD) was 1.3, with the average temperature rise being 152 ºC. Using a cosine distribution with a peak to edge ratio of 1.3 and an area equal to that of a constant 152 ºC rise, the following distribution was produced:

$$T_{increase}(r) = \frac{0.3 \cdot 152}{1 + 0.6/\pi} \cos\left(\frac{\pi r}{2b}\right) + \frac{152}{1 + 0.6/\pi} \tag{1}$$

where b is the outer radius of the fuel tube—1.0 cm. One final initial condition was the velocity of the coolant. This value was set at 0.35 m/s due to a quick analysis of the temperature rise experienced in the coolant if all added heat in the tube were removed in the allotted decay period.

A semi-infinite solution for a cylindrical rod was chosen as the appropriate analytic model for the analysis. This means that the radial direction was assumed to be finite, while the axial direction was assumed to be infinite. To accommodate a necessary approximation for the coolant (described in detail below), this model was slightly modified.

To begin, the differential heat equation in cylindrical coordinates was applied, using two necessary boundary conditions. Note that all temperatures are differential, which is a useful simplification in the boundary conditions—$\theta(r,z,t) = T(r,z,t) - T_{\infty}(z,t)$ where T is the fuel tube temperature, and T_{∞} is the coolant temperature. In all equations, α is the thermal diffusivity of the fuel material, b is the outer radius of the tube, k is the thermal conductivity (the subscript denotes the referenced material), and h is the heat transfer coefficient for the coolant at the convective boundary.

$$\frac{\partial^2\theta}{\partial r^2} + \frac{1}{r}\frac{\partial\theta}{\partial r} + \frac{1}{r^2}\frac{\partial^2\theta}{\partial\varphi^2} + \frac{\partial^2\theta}{\partial z^2} = \frac{1}{\alpha}\frac{\partial\theta}{\partial t} \tag{2}$$

$$\text{B.C. 1: } k_{fuel}\frac{\partial\theta}{\partial r} + h\theta = 0 \quad \text{at } r = b \text{ and } t > 0 \tag{3}$$

$$\text{B.C. 2: } \theta(r,z,t) = \theta_o(r,z,t) \quad \text{at t=0} \tag{4}$$

Boundary condition 1, Equation (3), gives the convective boundary condition at the interface. Boundary condition 2, Equation (4), is the initial temperature condition of the fuel.

Using these boundary conditions, the solution was found for Equation (2). Osizik (1993) derives this exact condition in *Heat Conduction, Vol.2* and his solution is given below. This solution was compared to a hand derivation then checked in the original differential equation to ensure accuracy. Note that this solution uses Bessel functions of the first kind.

$$\theta(r,z,t)=\sum_{m=1}^{\infty}\left[\frac{2\beta_m^2 e^{-\alpha\beta_m^2 t}J_0(\beta_m r)}{b^2\left(\beta_m^2+{}^{h}\!/_{k_{fuel}}\right)J_0(\beta_m b)}\int_0^b r' J_0(\beta_m r')\theta_o(r',z)dr'\right] \tag{5}$$

β_m denotes the eigenvalues for this solution, given by the following eigencondition.

$$-\beta_m J_1(\beta_m b)+{}^{h}\!/_{k_{fuel}}\,J_0(\beta_m b)=0 \tag{6}$$

As stated above, a simplification has been made to allow this eigencondition to be equal to 0. This comes about when allowing the coolant temperature to be zero, which can be achieved through the differential temperature substitution.

The final step was to include the coolant interface into the solution somehow, allowing for a changing heat sink. Since an analytic solution for this region was not easily attainable, a simple relationship of heat transferred across the boundary was used. This then yielded an equation for the temperature of the coolant as given below in Equation (7).

$$T_\infty(z+1,t)=T_\infty(z,t)+\frac{h\cdot b\cdot \delta z}{\dot{m}\cdot c_p}\left(T(b,z,t)-T_\infty(z,t)\right) \tag{7}$$

This approximation takes the heat transferred to the coolant from the tube and balances it with the inlet and outlet temperature of that node of coolant. Figure 3 gives a simple visualization of this system.

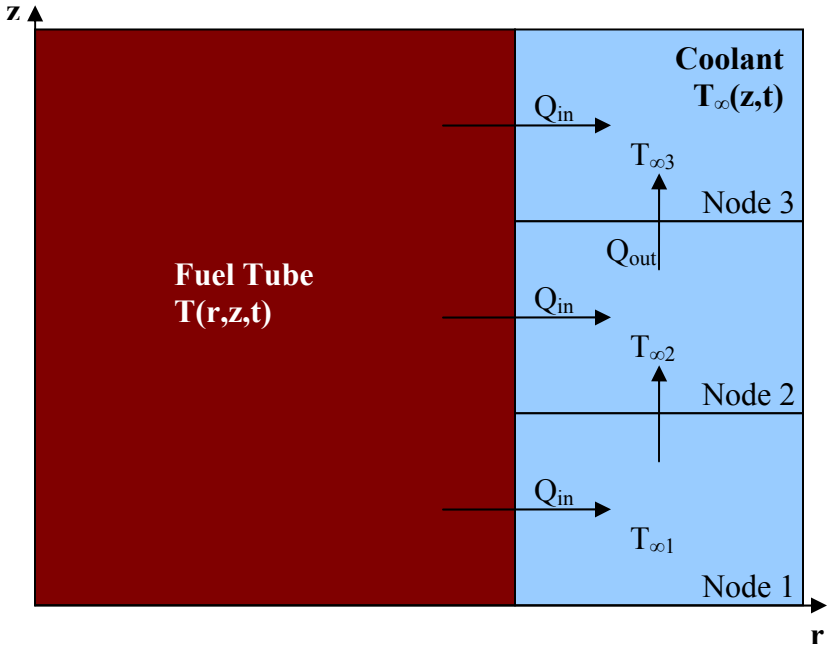

Figure 3: Heat Transfer Model

For this system to work, the approximation must modify the semi-infinite nature of the fuel tube model. Since the coolant channel has a finite length, given inlet temperature, and the outlet temperature is an output value, the analytic model would have to be changed to have start and end points. Although this would turn the model into a finite cylinder, the infinite solution was still used for two main reasons. First, the finite cylinder brings corners into the model, which could potentially cause singularities and problems. Second, since the coolant temperature can be calculated after the fact, this calculation does not have a large enough effect on the solution to warrant a new model. On that basis, the infinite model was used, adding a finite calculation at the back-end.

The calculation method for this interface became very important. First, the calculation of the radial profile in the fuel tube was calculated at a given time for the lowest axial position. In that calculation, the base coolant temperature was used. Once that profile was determined, the coolant temperature for the next node was modified using Equation (7). This was continued in the axial direction until the end of the model was reached.

Once complete, the model was programmed into Matlab to enable a large matrix of data to be compiled, giving radial, axial, and temporal dimensions. This also allowed an easy stacking of the pulses. At the given pulse period, the temperature inside the tube was increased by the aforementioned deposition distribution. It was assumed as an instantaneous rise since the amount of time for the radiation to increase the energy and temperature of the system was much smaller than the time scales used in this model. The fuel tube was then given time to decay using Equations (5) and (7) before another rise was added. This program ran until a convergence was met—defined as the centerline temperature at mid-height decaying to within 10 ºC of its value before the preceding pulse—or until a maximum number of pulses was reached.

Although the Matlab code will not be discussed in detail in this summary, one item to note is that in order to perform the integral in Equation (5), a Gaussian quadrature method of integration was used. Since the T_∞ in the equation becomes nodalized, it cannot be used in an exact integration. Also, Bessel functions behave in a way that is not easily approximated by usual numerical methods. The Gaussian quadrature used, however, was modified to further the accuracy of the model. The oscillatory nature of the Bessel functions produced zeros for the function in the interval of integration. Then, a predefined number of Gauss points were taken, and an approximation for the area under that portion of the curve was noted. All of these individual areas were them summed to give the total area under the curve in the interval.

Pertinent input information in Matlab is summarized below in Table 2. These inputs were consistent over all cases unless otherwise noted. Radial steps have only to do with what data points are calculated and recorded, while axial and temporal steps have an effect on the coolant nodalization.

Variable	Value
Number of Radial Steps	20
Number of Axial Steps	20
Number of Temporal Steps	5 per pulse period
Number of Gauss Points	5 per section
Max Number of Pulses	100 (200 for Standard Model)
Pulse Period (seconds)	10
Number of Fourier Series Iterations	150

Table 2: MatLab Modeling

Analytic Model Results

The optimized model had a fuel tube height of 6 m, radius of 1 cm, thermal conductivity in the actinide mixture of 1 W/m-K, and a specific heat in the mixture of 2380 J/kg-K. Figure 4 shows the temperature progression of the centerline at the axial center. The centerline temperature is the temperature of the actinide mixture in the center of each tube. This figure gives the temperature progression at the mid plane of the reactor for a tube that receives peak energy deposition. Each step rise on the graph represents the change in temperature after each fusion pulse, which at all times is equal to 152 ºC. The subsequent drop off represents how well the heat is removed. At the beginning of life, the temperature rose with little drop off. After about 300 seconds (30 pulses), the In-Zinerator was close to its equilibrium. The centerline equilibrium temperature appears to occur around 3500 K (3225 ºC).

This steady-state temperature is much too high, since the boiling point of LiF is about 1676 ºC. However, this analysis does give the design a point to work from. In future work, various techniques can be examined for reducing the centerline temperature—such as further geometry changes or decreases in multiplication.

Figure 5 gives the radial temperature profile of the standard model. As can be determined, the time taken before the profiles begin to get closer to repeating each other (the quasi-steady state situation) is extreme. The temperatures reached at that point are also extreme. Since every ten seconds an instantaneous pulse and temperature increase occur, there will be two temperatures per time step at those points. Positive and negative signs give the condition post- and pre-pulse, respectively.

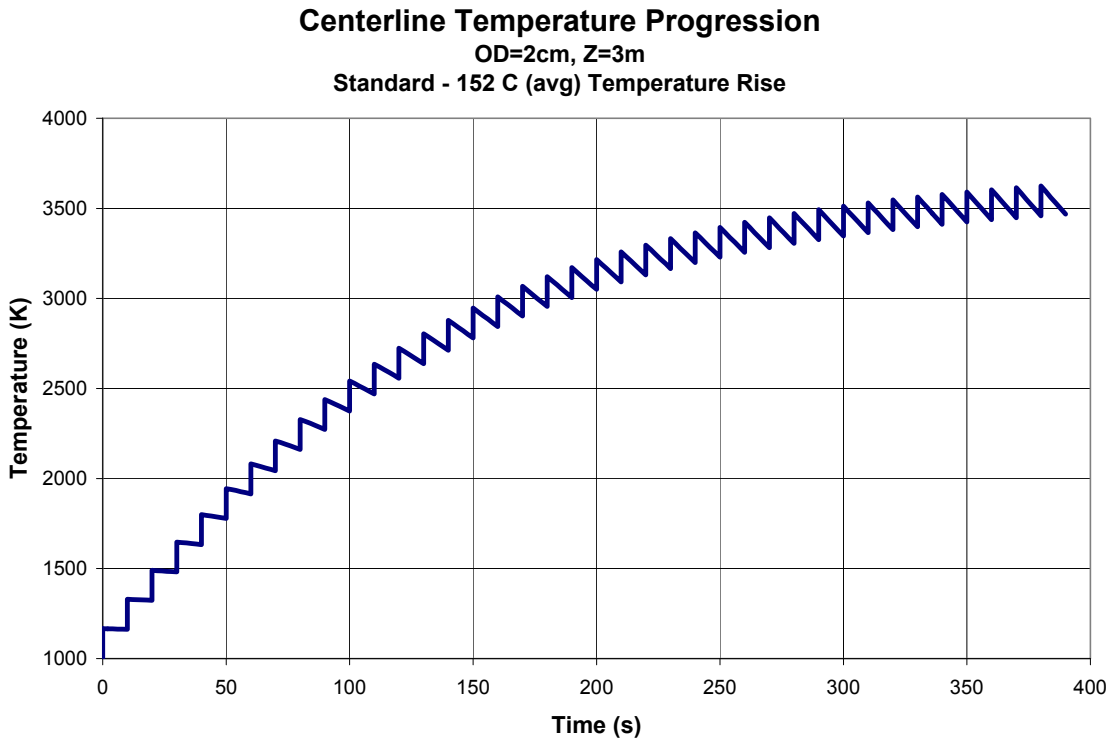

Figure 4: Actinide Mixture Temperature Progression at Beginning of Life

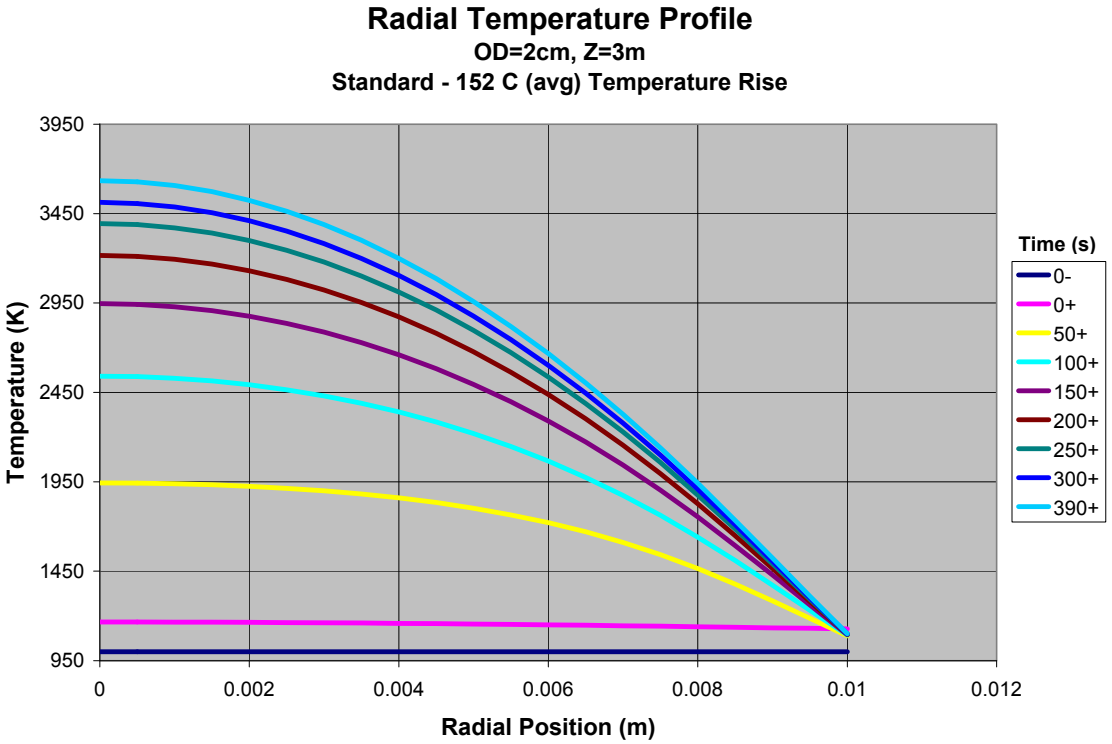

Figure 5: Radial Temperature Profile in the Tube

One of the difficulties with performing this analysis is that approximations for the specific heat and thermal conductivity of the actinide mixture were used. Until experimental data on these values can be obtained, it makes little sense to do a detailed parameterization study. However, it was found that the thermal conductivity of the actinide mixture had a strong influence on the steady-state centerline temperature—the higher the thermal conductivity, the lower the centerline temperature. Likewise, as the specific heat of the actinide mixture decreased, so too did the centerline temperature.

2.3 Aerosol Protection Scheme

The inner chamber wall requires protection from x-rays while allowing neutrons to pass through to the actinide blanket. A potential solution is to use a dispersal of solid or liquid particulates either suspended temporarily in a vacuum or falling very slowly through a low pressure gas. If the density of aerosols is high enough, the x-rays will be greatly attenuated before reaching the wall. This section will address the concept of a suspension of liquid aerosols.

By using droplets of liquid as a "shine shield," the x-ray energy may be significantly attenuated before reaching the first wall of the chamber. For this study the target energy was modeled as 10 MJ of x-rays in a cylindrical chamber with a height of 6 m and a radius of 2 m. Figure 6 illustrates the concept of an aerosol-protected chamber for the In-Zinerator actinide burner. The chamber first wall is shielded from direct line-of-sight to the target detonation and the subsequent x-ray release by a tin aerosol in an argon atmosphere of 30 Torr. Tin was chosen as the aerosol material because it is also the current candidate material for the recyclable transmission line (RTL). The schematic shows that a thin film could also be established as a last line of defense by having a portion of the aerosol impinging on the first wall.

An overall energy balance was used to determine the minimum requirements for the amount of tin needed in the chamber. This calculation assumed that the tin was heated from 325 to 2035 ºC (boiling at 30 Torr) for several different ending qualities (see Figure 7). The quality is defined as the ratio of the mass of vaporized tin to the total mass of tin. These values assume that the tin heats uniformly and does not contribute significantly to the overall chamber pressure. In reality, the temperature distribution will be higher in the center of the chamber and decay sharply towards the walls as the x-ray energy is attenuated. This calculation also ignores any temperature rise in the argon gas. Based on these values, the chamber may be protected by 23.5 kg of tin or less depending on the ending quality. This amount of tin translates into a rather sparse aerosol with a volume fraction of $\alpha = 5.93 \times 10^{-5}$ or less.

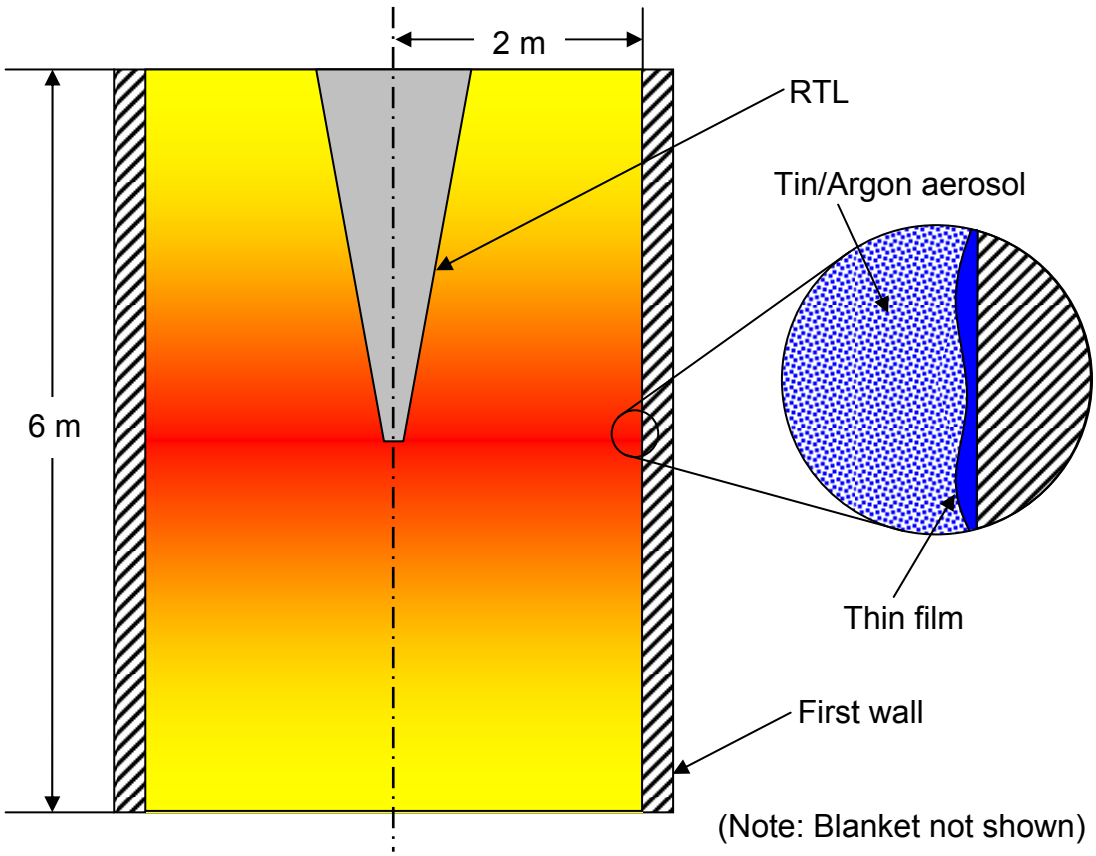

Figure 6: Aerosol Protection Concept

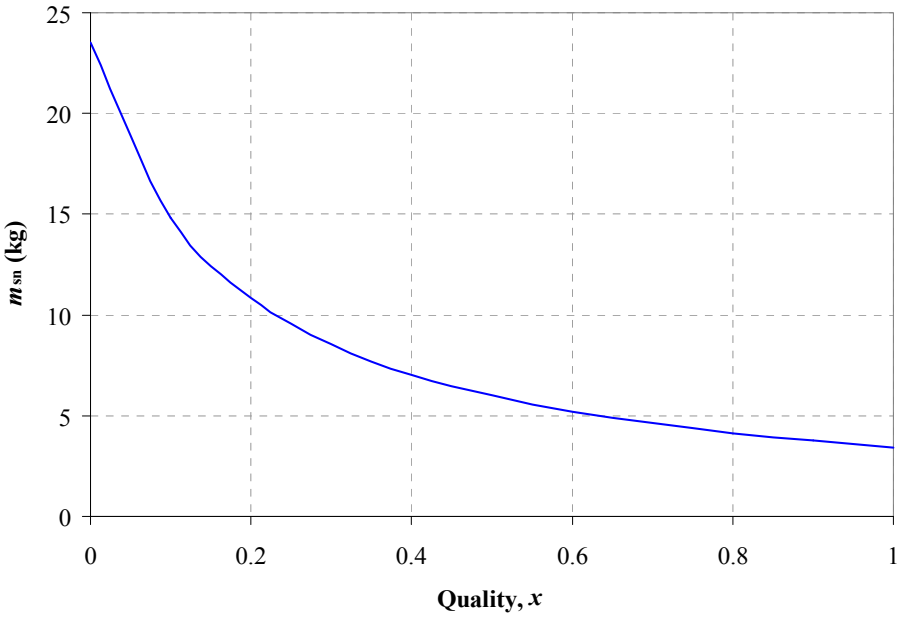

Figure 7: Minimum Mass of Tin Required to Absorb the X-ray Energy

The power required to deliver 23.5 kg of tin to the chamber is estimated next. The tin aerosol is delivered between shots at 10 second intervals, or a repetition rate of 0.1 Hz. Therefore, the mass flow rate is estimated at 2.35 kg/s. The pumping power required to inject the tin with an assumed pump efficiency of 0.8 and a system head of 60 m is 1.7 kW, a very small amount of power compared to the total power output of 3 GW.

Previous work was performed to estimate the radial energy deposition in an aerosol [10]. To simplify the geometry, these energy deposition calculations assumed a spherical chamber. The initial energy deposition into a spherical chamber with a radius of 2 m and protected by tin, $\alpha = 5.93 \times 10^{-5}$, and argon, P = 30 Torr, is shown in Figure 8. The region of constant energy density in the center of the chamber is due to a cutoff criteria of 3 keV/atom imposed in the model treatment. The calculated fraction of x-rays passing through the aerosol to the first wall is 0.006%, which would cause a negligible temperature rise in the first wall. A chamber protected by argon alone would require a pressure of 600 Torr to afford the same level of protection.

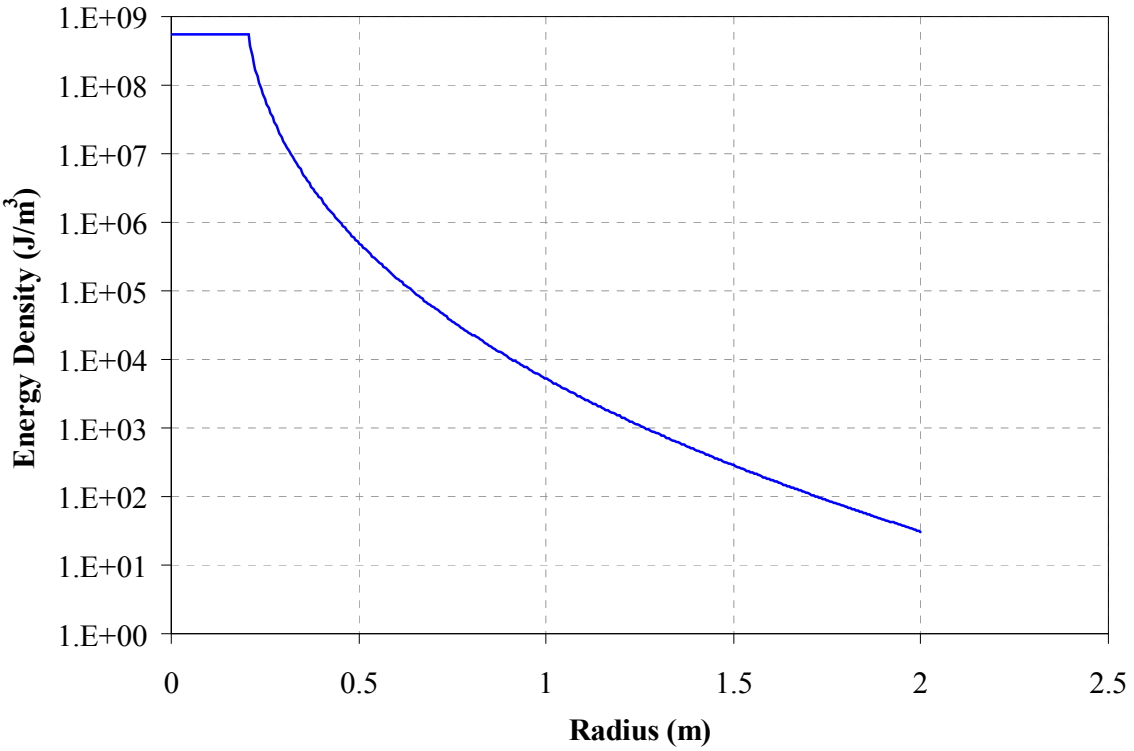

Figure 8: Energy Deposition as a Function of Radius in a Spherical Chamber Protected with Tin and Argon, $\alpha = 5.93 \times 10^{-5}$, P = 30 Torr

Further investigation is required to examine the temperature distribution and transient motion inside the chamber after the initial energy deposition. This problem would likely need to be simplified using a homogenized equivalent material, blending the properties of the gas and the liquid droplets. Otherwise, the disparate length scales of the droplets and the chamber radius

would translate into a computationally intense solution domain. The overall stress and temperature rise induced in the first wall are two important values that need to be resolved from these simulations.

2.4 Active Criticality Control

Over the lifetime of the In-Zinerator reactor, the energy multiplication will be greatly depressed because of the depletion of fissile material. This large drop in energy multiplication can be controlled by changing the composition of the fuel entering the reactor. The entire inventory of fuel is replaced daily; and by continually changing the composition of the fuel, specifically the Li enrichment and actinide fraction, the changes in energy multiplication over the lifetime of the reactor can be controlled. Changing the fuel composition, however, does not address the daily operation of the plant since the In-Zinerator is pulsed on the time scale of seconds and the fuel is replaced on the time scale of hours and days. This creates the need for active criticality control. Such a system must be able to control the energy released in each pulse of the In-Zinerator, on the time scales comparable to the pulsing time scale. The criticality of the reactor would need to be fine-tuned between pulses and able to be changed in seconds. This is the motivation of the leakage rods; rods which would be able to be inserted or retracted quickly to depress or increase the energy released.

Leakage Rods

The purpose of the leakage rods is to allow some of the neutrons to leak from the system by preventing their return from the outer lead coolant region. This decreases the energy released by preventing the escaped neutrons from causing more fission events. The leakage rod design is an air-filled tube that can be inserted into the lead coolant, displacing the lead. Since air reflects fewer neutrons than lead, the reflector becomes less effective, letting more neutrons escape and depressing energy multiplication. The insertion of leakage rods was modeled in MCNP by decreasing the lead reflector density (consequently increasing the mean free path of the neutrons and decreasing the amount of neutrons interacting with the reflector).

Figure 9 shows the MCNP result of varying the reflector density. As the density decreases (mimicking insertion of the leakage rods), the multiplication decreases. The energy multiplication with the nominal density of lead drops to 61% of this high by completely removing the outer lead coolant. The error bars are calculated using MCNP statistics. Realistically, only a portion of the lead coolant can be displaced with leakage rods.

Figure 10 shows the effect that the leakage rods have on k_{eff}. With no outer coolant the k_{eff} drops 0.024 from the nominal case, though the change would be less for a more realistic displacement. Although this is a small value, it can allow the leakage rods to control criticality if a small reactivity insertion occurs. This would allow for fine tuning of the energy multiplication for daily operation while changes in fuel composition can account for larger drops in energy multiplication over the lifetime of the reactor.

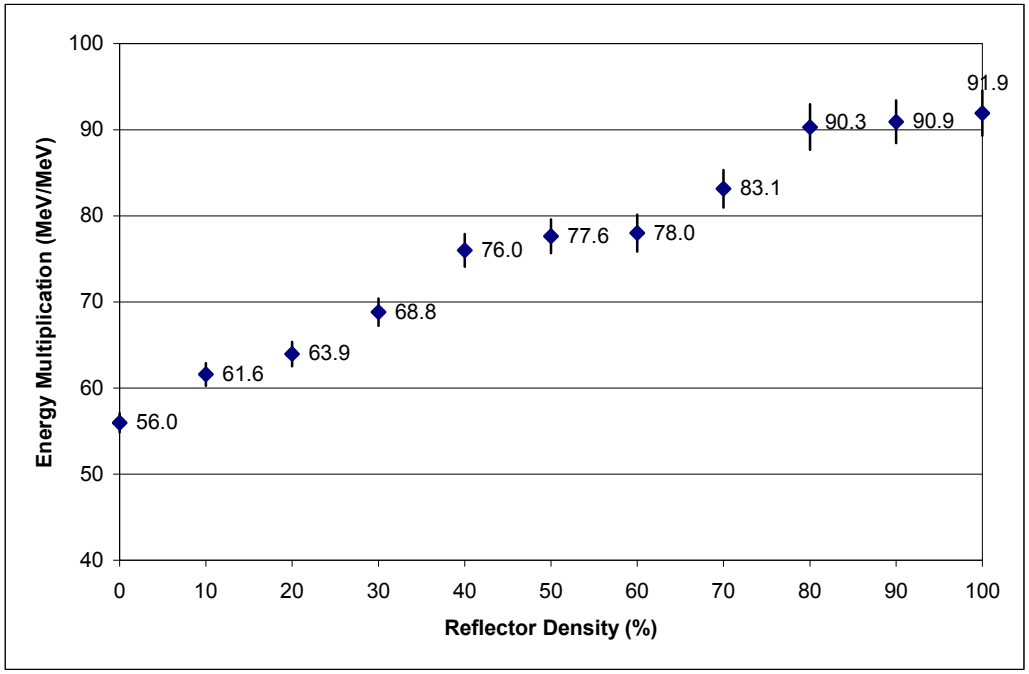

Figure 9: Energy Multiplication as a Function of Lead Density

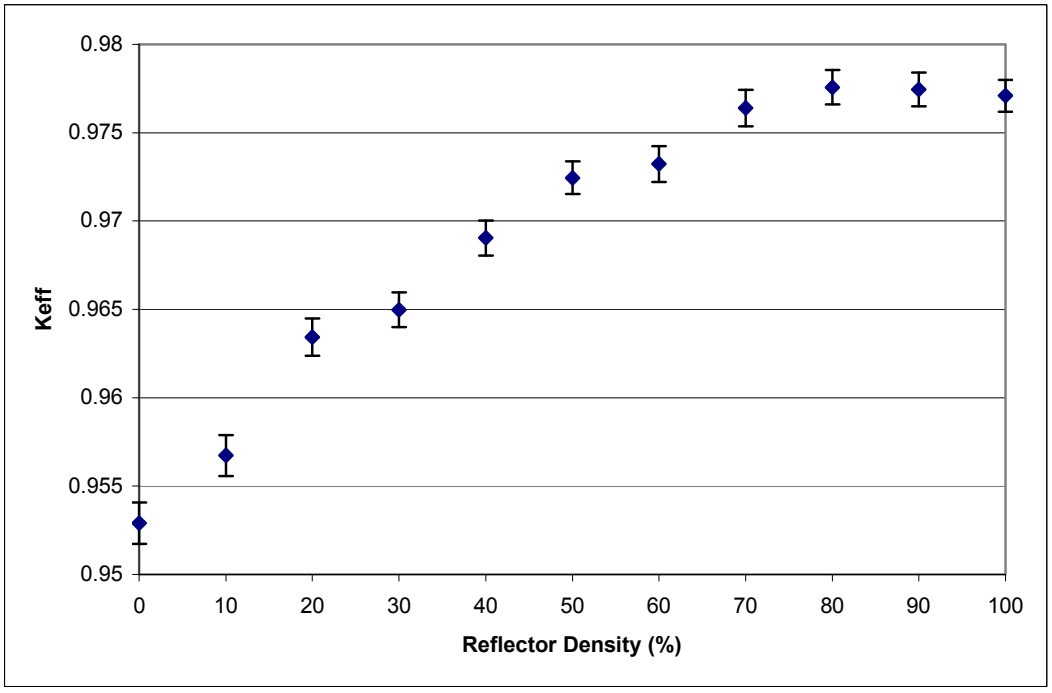

Figure 10: k_{eff} as a Function of Lead Density

3.0 Transmutation Analysis

3.1 Transmutation Modeling

The MCise computer code has been used to perform transmutation and burnup calculations for the In-Zinerator. The background and theory of MCise within the scope of the In-Zinerator were thoroughly described in Reference 1 and will be omitted here. Parameters in the analysis methodology of the current study are the same as those from last year except that now the feed stream changes slightly.

Model Description

The MCise model contains two control volumes representing the reactor core and the fission product extraction. The reactor core is characterized by the average neutron flux that the eutectic fuel experiences. This neutron flux is calculated by MCNP. For the purpose of this analysis, a residence time of 1 day in the reactor was chosen corresponding to the ability to process all inventory in a day in the fission product (FP) extraction step. The residence time of the FP extraction represents a processing period of the fuel and was assumed to be zero.

All of the flow leaving the reactor core goes to the FP extraction process, but the flow leaving the FP extraction process is divided into two streams based on the atomic species. All fission products and all non-actinide isotopes except Li and F flow to the sink; and all actinides, Li, and F are returned to the reactor core. This model was chosen to represent an ideal separations process, and the flow distribution of each species was adjusted to represent the real separations efficiencies. The extraction of all non-actinide isotopes keeps the amount of fissionable poisons in the system at acceptable levels.

As in any fissile system, a calculation of the long-term isotopics requires a tight coupling between the neutron transport calculation and the changing isotopics. In this system, justified in part by the constant replenishment of TRU fuel, the system was modeled with a constant neutron flux (both in magnitude and energy spectrum). The neutron flux at the beginning of operation was obtained from MCNP and normalized to 3000 MWth. It is shown in Figure 11.

The assumption of a constant neutron flux was justified by plotting the ratio of the energy multiplication and the total flux as a function of time. According to the Figure 12, the plot of the energy-flux ratio is not perfectly constant but it is only very slowly decreasing with time.

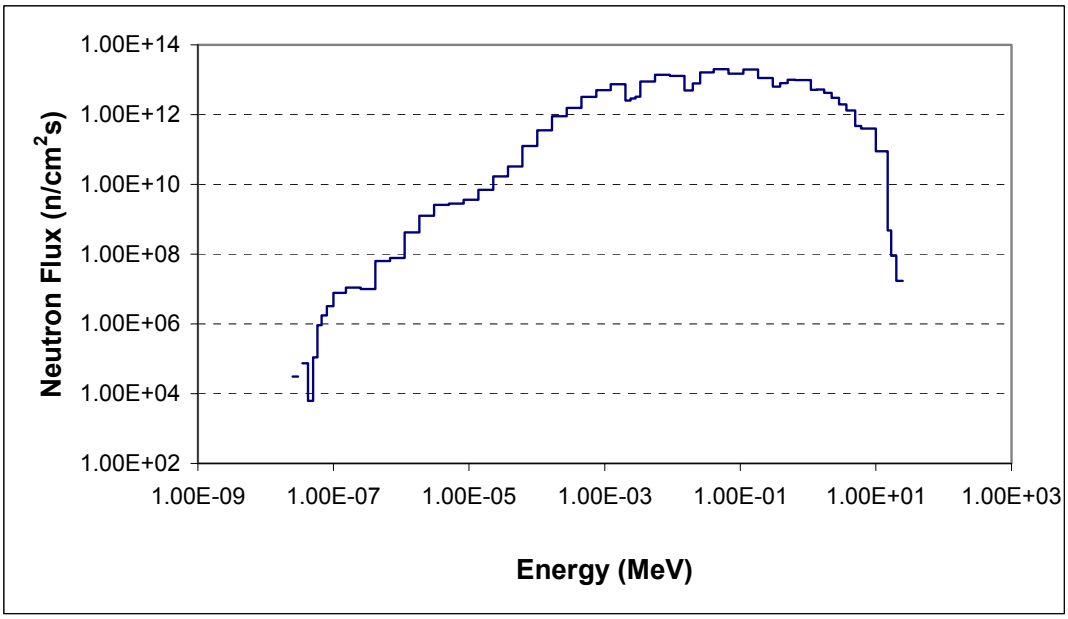

Figure 11: In-Zinerator Neutron Spectrum

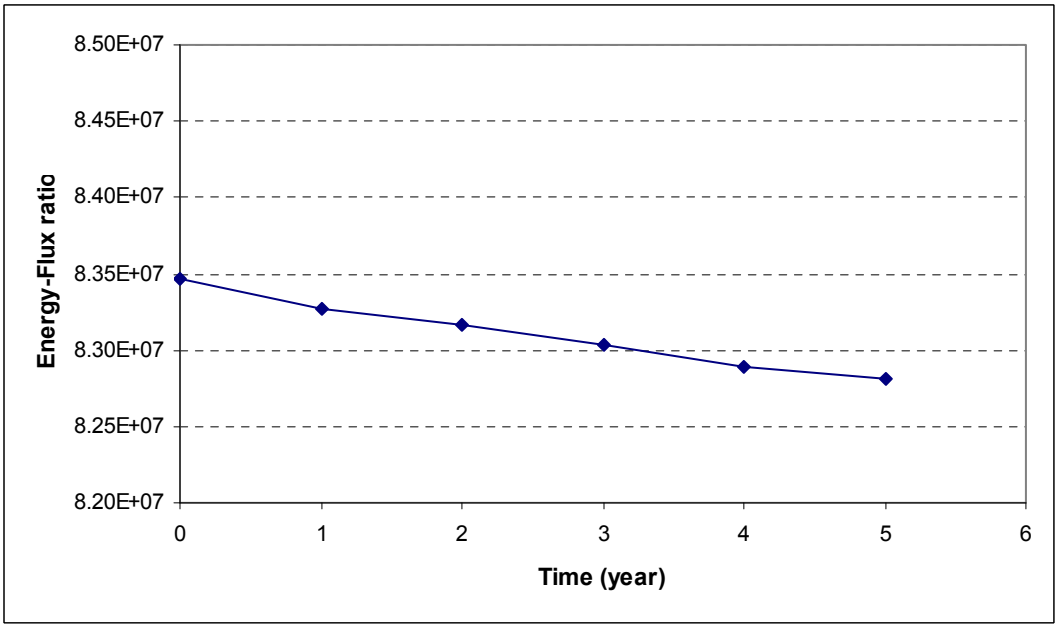

Figure 12: Energy-Flux Ratio vs. Time

Actinide Loading

The initial actinide loading in the blanket was 15% in the eutectic form of $(LiF)_{0.85}(AnF_3)_{0.15}$. Fresh actinides were assumed to be added to the system during the course of operation to keep

the multiplication constant. If the replenishment stream was kept constant with time, the result was a gradual decrease in multiplication with time because the isotopes with the highest fission cross-section burned up faster than they were being added. Therefore, it was assumed that the feed rate of the replenishment stream would be designed to result in a gradual increase of the actinide fraction as a slow long-term control mechanism in the reactor. Fission products were assumed to be removed quickly from the system. An iterative process between MCise and MCNP was used to determine an appropriate feed rate, on 5-year increments, to ensure a constant energy multiplication.

Actinide replenishment in this fashion should be reasonable in a real system. Assuming that the actinides are delivered to the In-Zinerator in the fluoride form, the change in concentration is accomplished simply by changing the amount of LiF added to form the eutectic. However, the reality of the chemistry of this eutectic process is uncertain since these mixtures have not been created in a laboratory yet. Future work will need to examine these mixtures in more detail.

3.2 TRU Burner Calculation

Initially, the In-Zinerator was loaded with 1.056×10^5 kg of a lithium fluoride eutectic constituted with actinide fluorides $(LiF)_{0.85}(AnF_3)_{0.15}$. The Li-6 enrichment was 3%. Isotopic distributions of the initial core loading and the feed are given in Table 3.

Isotope	Initial Core Loading (atomic fraction)	Feed Stream (atomic fraction)
Li-6	0.01109	-
Li-7	0.35848	-
F-9	0.56522	-
Np-235	1.000e-15	1.533e-14
Np-236	4.772e-09	7.316e-08
Np-237	0.00479	7.345e-02
Np-238	2.026e-12	3.107e-11
Np-239	1.174e-09	1.800e-08
Pu-236	1.000e-15	1.533e-14
Pu-237	1.000e-15	1.533e-14
Pu-238	0.00174	2.671e-02
Pu-239	0.02963	4.544e-01
Pu-240	0.01713	2.627e-01
Pu-241	0.00060	9.218e-02
Pu-242	0.00374	5.734e-02
Pu-243	1.000e-15	1.533e-14

Isotope	Initial Core Loading (atomic fraction)	Feed Stream (atomic fraction)
Pu-244	7.214e-07	1.106e-05
Am-241	0.00601	9.218e-02
Am-242	1.060e-05	1.626e-04
Am-243	0.00134	2.061e-02
Cm-241	1.000e-15	1.533e-14
Cm-242	2.575e-08	3.948e-07
Cm-243	1.799e-06	2.758e-05
Cm-244	0.00013	2.105e-03
Cm-245	5.643e-05	8.652e-04
Cm-246	1.259e-05	1.931e-04
Cm-247	2.433e-07	3.731e-06
Cm-248	2.793e-08	4.282e-07
Bk-249	1.000e-15	1.533e-14
Cf-249	1.000e-15	1.533e-14
Cf-250	1.000e-15	1.533e-14

Table 3: Core Loading and Refueling

The first MCise calculation concentrated on the first five years of operation where the total TRU fuel supplied to the system over this period was 5560 kg. This amount was determined solely based on the expected total actinides being burned to produce roughly 3000 MWth. The thermal outputs at different times are shown in Figure 13.

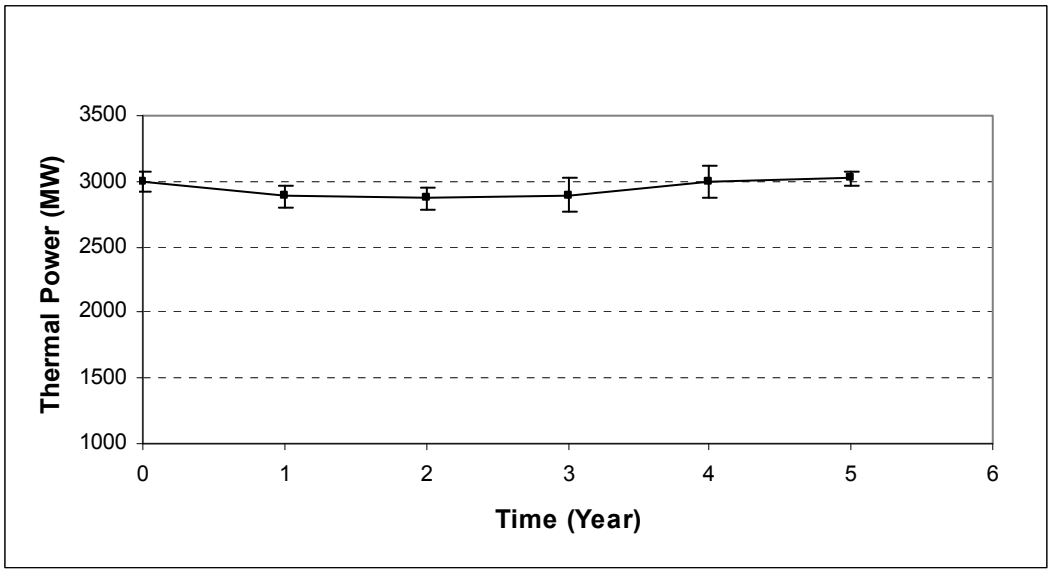

Figure 13: Thermal Power vs. Time

With the total TRU feed of 5560 kg, or 3.05 kg/day, the thermal outputs always remained within 5 percent of the desired energy output. Properly inserting or removing leakage rods in the reflector region could be used to perform a fine adjustment on the actual energy output. The tritium breeding ratio was between 1.4 and 1.6 at all times. The actinide concentration in the system slowly increased from 15 percent at the beginning of life to about 15.47 percent after five years.

Detailed time-dependent isotopic inventories of materials in the In-Zinerator were obtained from the MCise calculation. A total of 23 actinides and the sum of all fission products were plotted (See Figure 14). The plot groups elements by the same color. Pu (shown in red) makes up the majority of the actinide mixture, and most of these isotopes did not change considerably. The Np isotopes (shown in yellow) remained almost constant with time. All Am isotopes (shown in blue) except Am-242m also did not change significantly and leveled out after about 10 months. Some isotopes of Cm, Bk, and Cf rose considerably with time. These isotopes accumulated in the system because their fission rates were much lower than their feed rates.

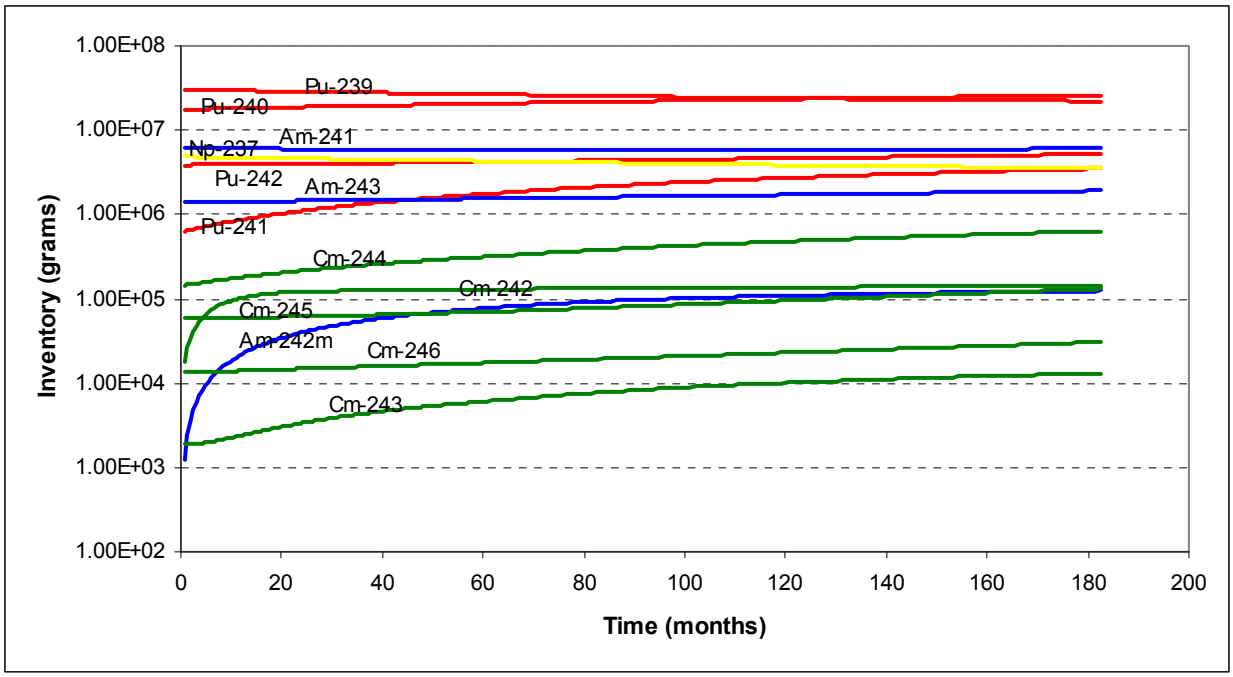

Figure 14: Actinide Inventory in the First Fifteen Years

The burnup/buildup rates of isotopes in the TRU feed at five years are shown in Table 4. The positive values in the table represent a net burn, while the negative numbers indicate those isotopes that were building up. Summing over all of the isotopes, there was a net burn of 3.62 kg/day at five years with a power output of 3020 MW_{th}.

Figure 15 shows the burnup/buildup rates for the most important actinides. During this early time in the reactor life, ^{237}Np, ^{239}Pu, and ^{241}Am burned up well. On the other hand, ^{238}Pu and ^{241}Pu were building up in the system. The rest of the isotopes changed very slowly.

The same modeling strategy was used to determine additional fuel feed for the next two 5 year time steps. Total fuel feed was adjusted every five year. The total fuel feed for the first five years was 5563 kg. The subsequent total fuel feeds during the next ten years were 6446 kg and 7266 kg., respectively. The thermal outputs were always within five percent of the target thermal output as shown in Figure 16. Error bars indicate 1σ statistical error of each data point.

Isotope		Burnup/ *Buildup* (g/d)	Isotope		Burnup/ *Buildup* (g/d)
Np	235	*-5.64e-5*	Am	241	541
	236	9.08e-4		242	30.4
	237	536		243	*-18.2*
	238	2.19	Cm	241	*-8.59e-5*
	239	7.07e-3		242	*-4.94*
Pu	236	*-4.80e-3*		243	*-2.37*
	237	0.0200		244	56.3
	238	*-626*		245	*-6.74*
	239	3410		246	*-0.862*
	240	12.8		247	*-0.233*
	241	*-351*		248	*-0.0137*
	242	6.35	Bk	249	1.23e-3
	243	33.3	Cf	249	*-9.53e-4*
	244	0.0234		250	*-1.41e-5*

Table 4: Actinide Buildup/*Burnup* Rates

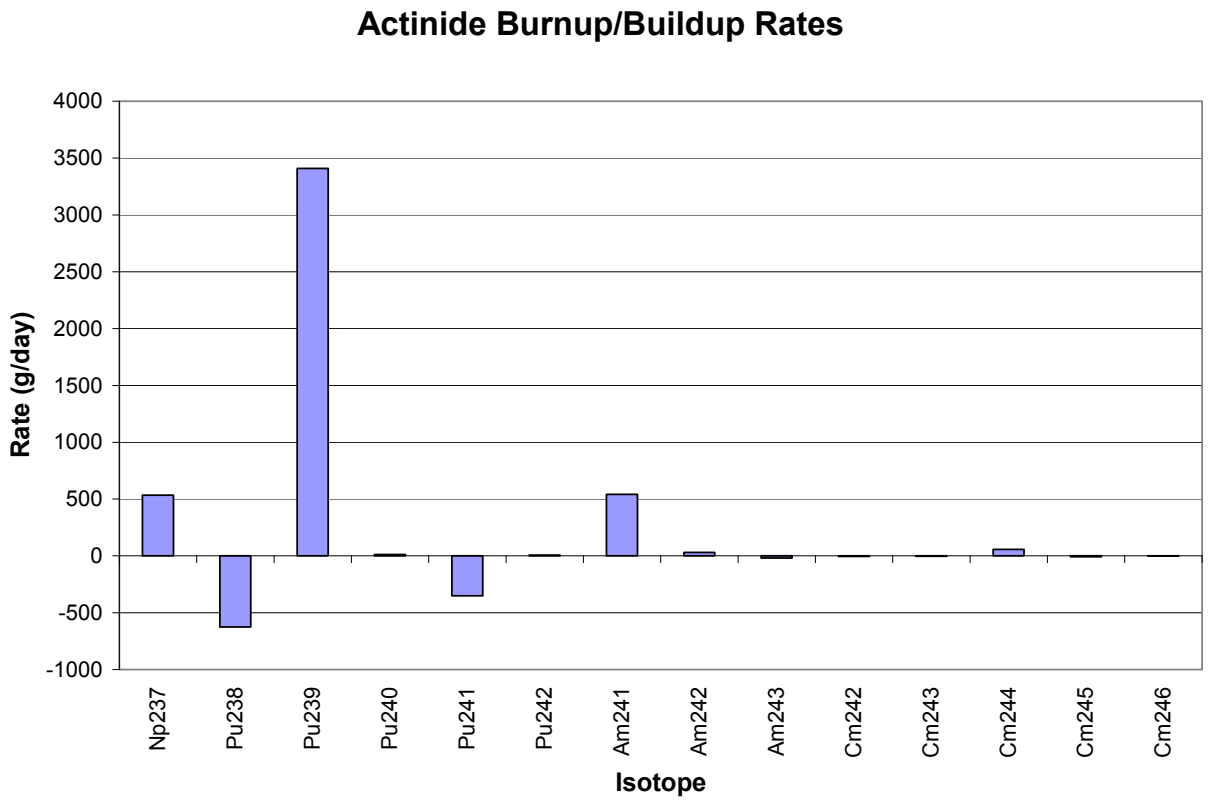

Figure 15: Actinide Burnup/Buildup in the First Five Years

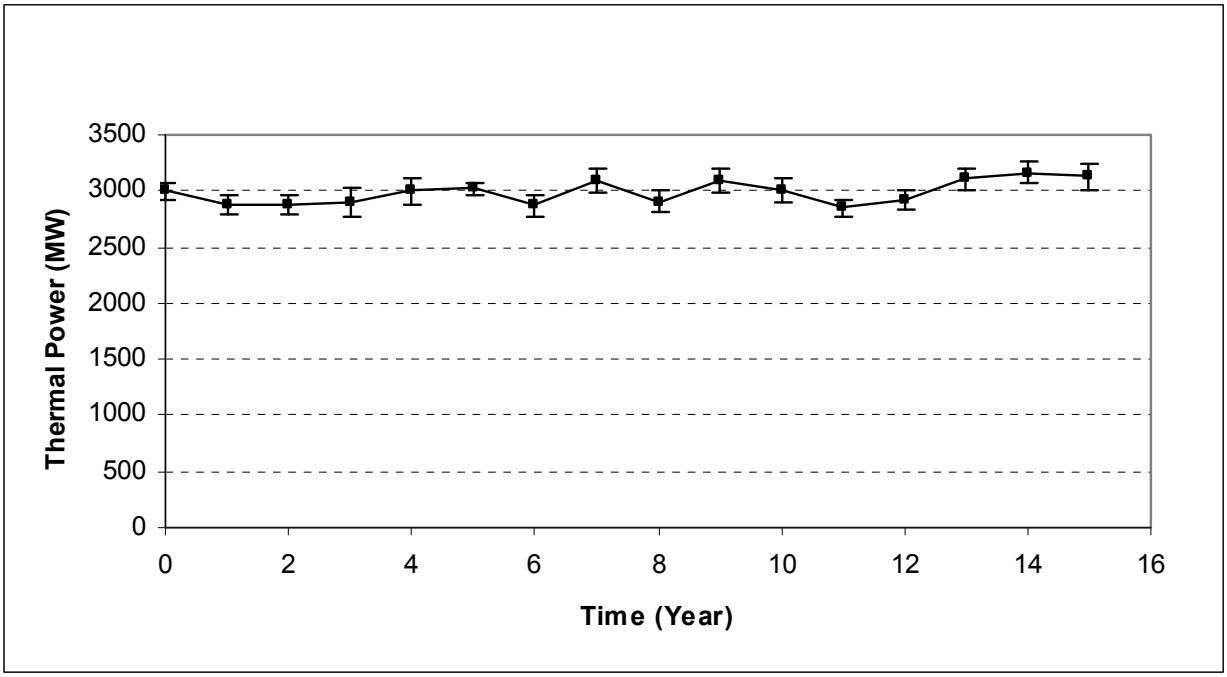

Figure 16: Thermal Output During the First Fifteen Years of Operation

At the end of fifteen years, the *In-Zinerator* produced 3125 MWth and with a total removal rate of actinides of 3.81 kg/day. The system continued to burn up ^{237}Np, ^{239}Pu, and ^{241}Am while accumulating ^{238}Pu and ^{241}Pu. These burnup/buildup characteristics were the same as the early time. The actinide concentration in the system was expected to increase over time since the feed rate was higher while the total burnup rate remained about the same. Figure 17 shows the actinide concentration and the feed rate over time. The actinide concentration increased in a piecewise linear fashion from 15% at the beginning of operation to about 16.8% at the end of fifteen years. It is possible to estimate the actinide concentration at forty years of operation by extrapolating the current results to forty years. The extrapolated actinide concentration at forty years is about 20% which is well below the (assumed) eutectic limit of 33%. A large difference between these two values implies a large reactivity control from varying actinide concentration.

Tritium breeding ratio during this period gradually decreased from 1.65 to 1.05 at the end of fifteen years (See Figure 18). This decreasing trend suggested that additional lithium-6 would need to be added to the system, which can be explored in future work.

The Pu vector changes significantly during the life of the reactor. Figure 19 shows the isotopic distribution of Pu in the TRU feed from spent nuclear fuel (which also represents the distribution in the In-Zinerator at the beginning of life). Pu-239 dominates the distribution. Figure 20 shows the Pu vector at the end of 15 years of operation. Pu-240 builds up significantly while the Pu-239 burns up well. This pattern will continue to have implications on the blanket fueling in the time frame beyond 15 years.

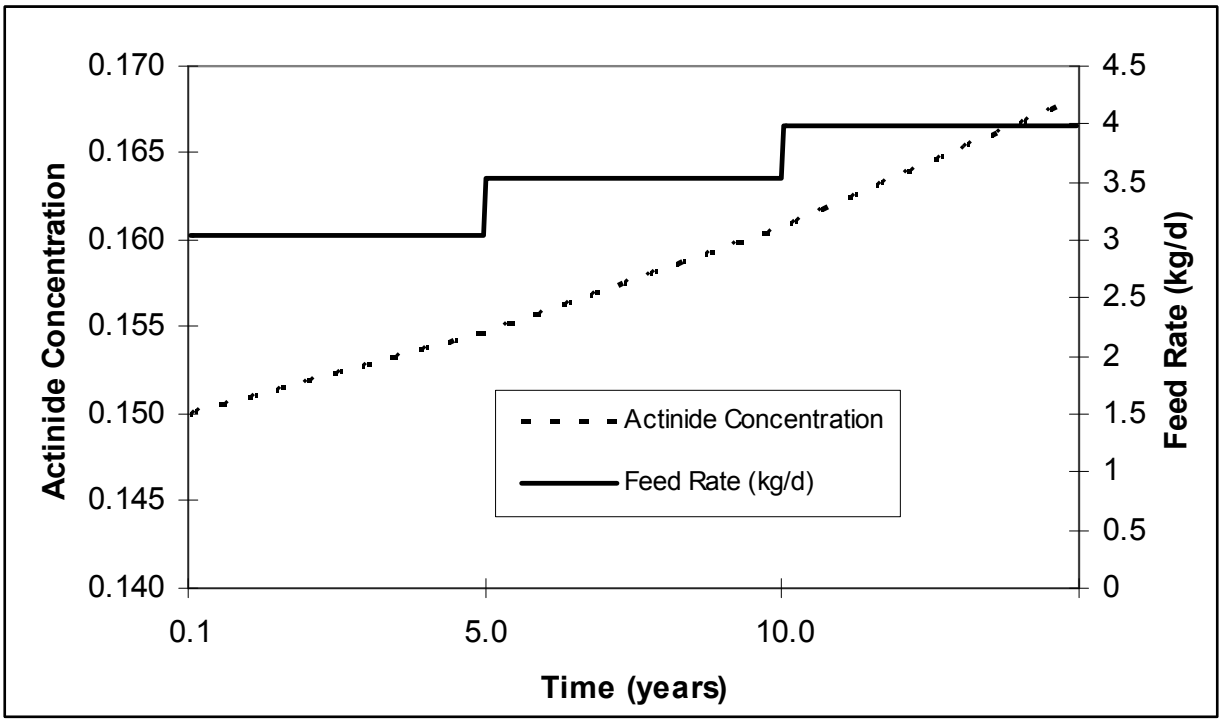

Figure 17: Actinide Concentration vs. Time

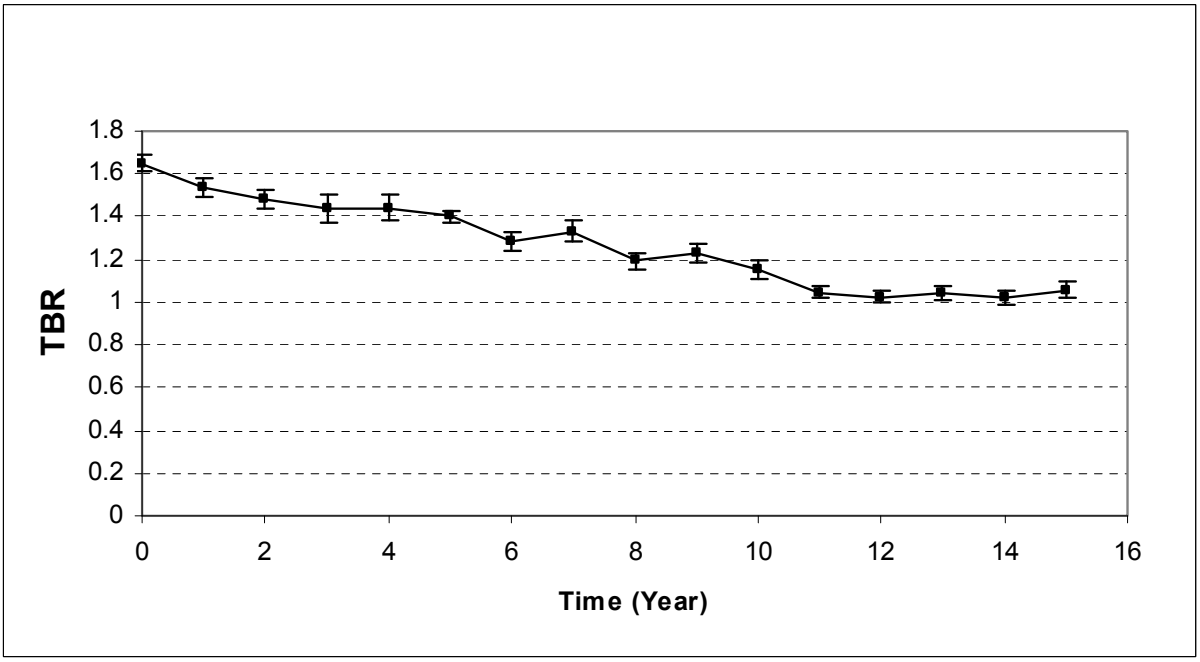

Figure 18: Tritium Breeding Ratio vs. Time

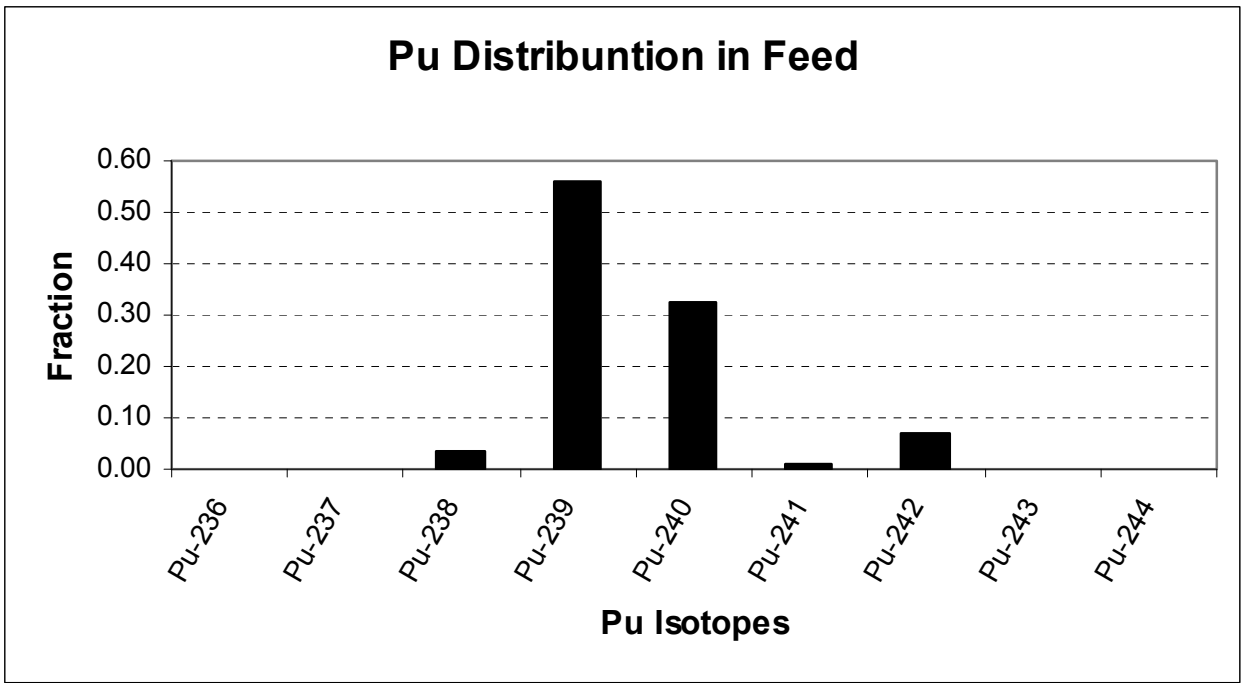

Figure 19: Beginning of Life Pu Vector

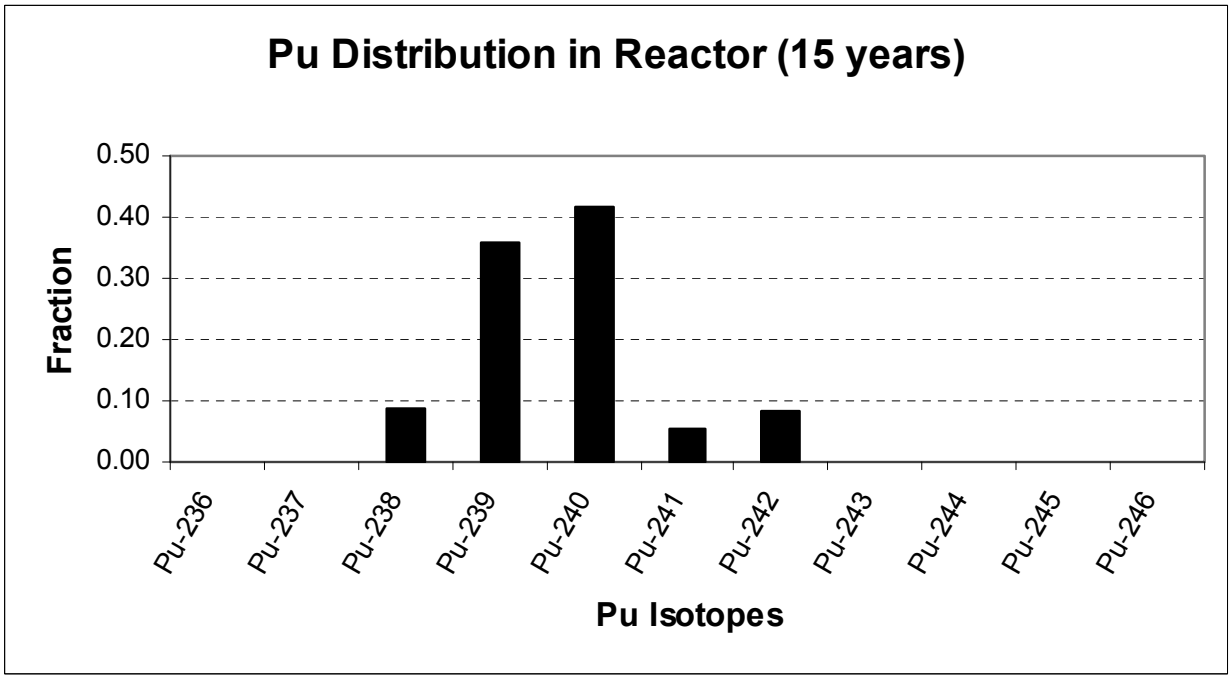

Figure 20: Pu Vector at Fifteen Years

4.0 Economics

Related work has examined the economics of the In-Zinerator concept as it fits into the entire nuclear fuel cycle [11]. The Sandia GenSim model is an economic tool for comparing the cost of electricity from various energy sources. This model was extended (as described in reference 11) to compare the economics of different nuclear fuel cycles. The following six fuel cycles are compared in the model:

1. Historical – The existing light water reactor (LWR) fleet
2. LWR MOX – Thermal recycle of plutonium in the existing LWR fleet
3. GNEP – A combination of existing LWRs and fast reactors (FR) used for complete TRU burning
4. In-Z – A combination of existing LWR and In-Zinerators used for complete TRU burning
5. GNEP MOX – A combination of thermal recycle of actinides in existing LWRs with FRs used to burn all left-over actinides
6. In-Z MOX – A combination of thermal recycle of actinides in existing LWRs with In-Zinerators used to burn all left-over actinides

Any type of advanced burner reactor is likely to cost more than a LWR. The technological complexity of fast reactors and fusion-driven waste burners will lead to higher costs, so they are unlikely to be economically competitive for producing electricity alone. However, they also burn up actinide wastes. The key, then, is to determine what our society is willing to pay to minimize the amount of long-lived nuclear waste in need of disposal. The different fuel cycles listed above examine ways to decrease the number of fast reactors or In-Zinerators needed to bring down the overall fuel cycle cost of electricity as low as possible.

A screen shot of the GenSim model that compares the various nuclear fuel cycles is shown in Figure 21. In this figure, the top graph shows the fleet averaged cost of electricity for the different fuel cycles. The different colors represent which portion of the cost comes from the various facilities in the fuel cycle. The bottom graph shows how long it will take for each fuel cycle to fill up the Yucca Mountain Repository. The tables in the middle show the key cost assumptions which can be changed in the model.

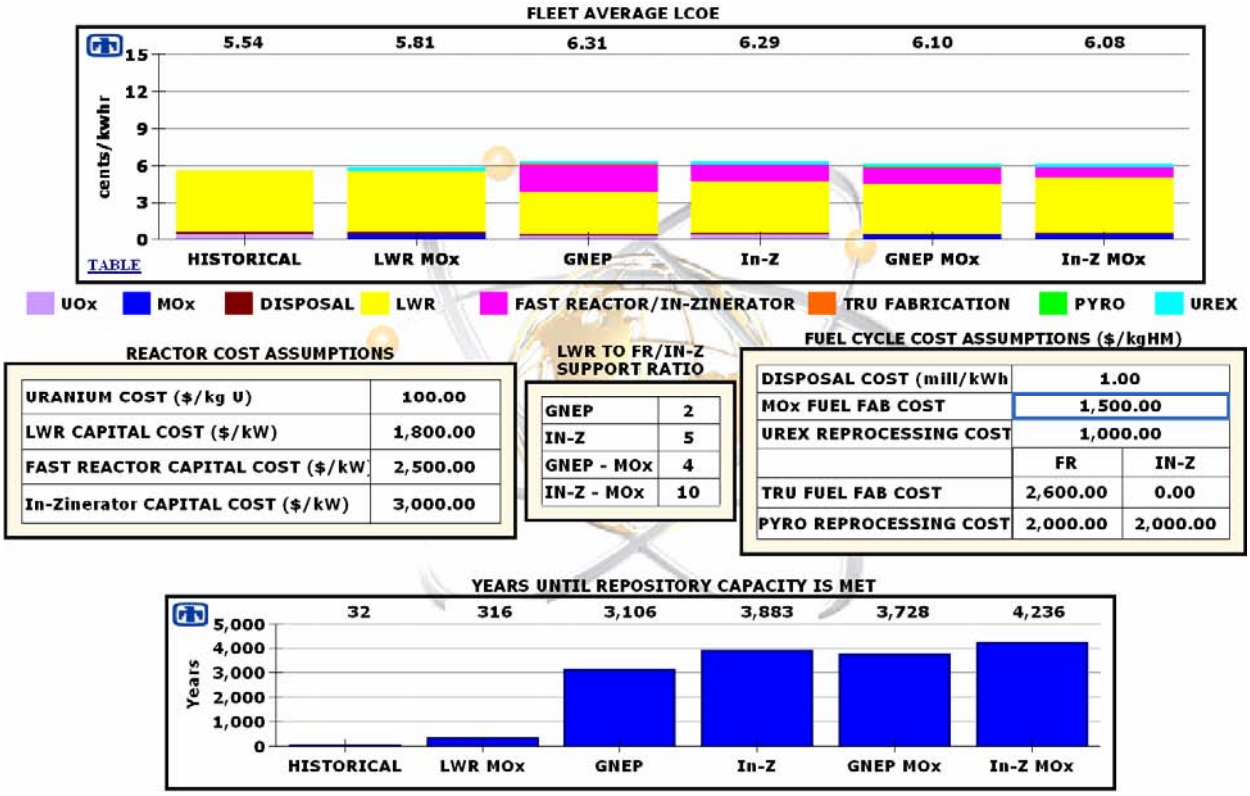

Figure 21: GenSim Model

The first key point that can be easily seen is that all advanced fuel cycles that require reprocessing and transmutation will cost more than the historical once-through cycle, which means these options are only going to occur if a policy decision is made by the government to fund it. Reprocessing and advanced burners are expensive, so they will only add to the cost of the overall fuel cycle. However, since the true economic and political costs of a waste repository are not known well, society may find that it is worth the extra cost to keep from needing to build additional repositories.

There also does not appear to be any major cost difference between using fast reactors and In-Zinerators to burn actinides. It was assumed that an In-Zinerator would cost about $500 per kWe more to build than a fast reactor, but the better support ratio of the In-Zinerator makes up for the higher individual cost. In other words, each unit may cost more to build, but fewer In-Zinerators that Fast Reactors are required to burn all the TRU generated by LWRs.

The last two fuel cycles show that engaging in limited MOX recycle in thermal reactors followed by actinide destruction in either fast reactors or In-Zinerators can decrease the overall cost of the fuel cycle by limiting the number of fast units. However, the least expensive of the advanced fuel cycles is thermal recycling of TRU, and both fast reactors and the In-Zinerator will be unlikely to compete. The penalty with thermal recycle is that it does not reduce the waste significantly compared to fast systems.

The current political environment may not yet be ready for actinide burners, and technologically it does represent a large step. It will likely make much more sense to first recycle actinides in existing LWRs. This approach allows for more time to demonstrate and bring down costs of actinide burning in fusion systems or fast reactors. However, eventually fast systems will be required to burn up all the left-over actinides from thermal recycle. It would be advantageous to start a research path now that leads to a demonstration unit so that a full-scale unit is ready when the fuel cycle demands it.

5.0 Conclusion

The FY07 In-Zinerator baseline design has addressed many of the engineering issues of the system that were raised in the previous year. The current design is more realistic, but there are still a number of science and engineering issues that need to be resolved in future work.

The greatest change in the design was to decrease the actinide loading in the fuel mixture while spreading out the fuel region. At the same time, the number of fuel tubes increased and the tube diameter decreased. This change kept the radiation damage on all tubes below 50 dpa after 40 FPY. In addition, the fuel region was offset from the first wall slightly to keep the radiation damage to the first wall below 50 dpa after 40 FPY as well.

This geometry change also decreased the temperature rise in the coolant to 152 ºC after each shot. However, this temperature rise may still be too high to safely engineer around. The steady state centerline temperature in the actinide tubes was found to be 3225 ºC and occurred after about 30 pulses. Again, this temperature is too high. Any potential future work will need to modify the design to achieve acceptable temperature rises.

The first wall was found to be adequately protected from x-ray damage through the use of aerosol protection. About 23.5 kg of tin in an aerosol form per shot was adequate for absorbing the x-rays from the fusion target to prevent damage to the first wall. The aerosol volume fraction was $\alpha = 5.93 \times 10^{-5}$.

The new In-Zinerator design is better able to keep the multiplication of the blanket constant with time. The actinide loading starts at 15% and needs to be gradually increased to 20% by the end of 40 FPY of operation. The actinide burnup rate is about 1320 kg/yr. Fine-tuning of the multiplication can be achieved with air-filled leakage rods that can slightly adjust the k_{eff} of the system.

6.0 References

1. B.B. Cipiti et al., "Fusion Transmutation of Waste: Design and Analysis of the In-Zinerator Concept," SAND2006-6590 (November 2006).
2. "Final Environmental and Impact Statement for a Geological Repository for the Disposal of Spent Nuclear Fuel and High-Level Radioactive Waste at Yucca Mountain," Nye County, Nevada, U.S. Department of Energy, Office of Civilian Radioactive Waste Management, DOE/EIS-0250 (February, 2002).
3. "Total System Performance Assessment, Viability Assessment of a Repository at Yucca Mountain, Vol. 3," TRW Environmental Safety Systems, Inc., Las Vegas, NV (Sept. 10, 1998).
4. D. Benin, "Thermal Conductivity of LiF NaF and the Ziman Limit," *Physical Review B*, **5**(6), 15 (March 1972).
5. R.E. Stoller & L.R. Greenwood, "An Evaluation of Neutron Energy Spectrum Effects in Iron Based on Molecular Dynamics Displacement Cascade Simulations," Computation Physics Research and Development Division, Conference: 19th ASTM International Symposium on the Effects of Radiation on Materials, Seattle, WA (June 16-18, 1998).
6. Steven J. Zinkle, "Fusion Material Science: Overview of Challenges and Recent Progress," *Physics of Plasmas*, **12** (April 18, 2005).
7. D.S. Gelles, G.L. Hankin & M.L. Hamilton, "The Consequences of Helium Production on Microstructural Development and Deformation Response in Isotopically Tailored Ferritic Alloys," *Journal of Nuclear Materials*, **251**, 188 (1997).
8. R. Lindau, A. Moslang, D. Preininger, M. Rieth & H.D. Rohrig, "Influence of Helium on Impact Properties of Reduced-Activation Ferritic/Martensitic Cr-Steels," *Journal of Nuclear Materials* **271-272**, 450 (1999).
9. D.S. Gelles, "On Quantification of Helium Embrittlement in Ferritic/Martensitic Steel," *Journal of Nuclear Materials***, 283-287**, 838 (2000).
10. C.W. Morrow et al., "Roadmaps and Containment Concepts for Early Z-Pinch Fusion Applications," SAND 2007-2923 (May 2007).
11. T.E. Drennen & W. Kamery, "The Long Term Economic Outlook for Nuclear Power," to be published.

Distribution

2 Paul Wilson
University of Wisconsin
1500 Engineering Dr.
Madison, WI 53706

2 Pavel Tsvetkov
Department of Nuclear Engineering
129 Zachry Engineering Center, 3133 TAMU
Texas A&M University
College Station, TX, 77843-3133

1 Tom Drennen
Hobart & William Smith Colleges
314 Stern Hall
300 Pultney St.
Geneva, NY 14456

1 MS 0736 John Kelly, 6770
3 0748 Ben Cipiti, 6763
1 0748 Gary Rochau, 6763
2 1186 Tom Mehlhorn, 1674
1 1193 Dan Sinars, 1673
1 9018 Central Technical Files, 8944 (electronic)
1 0899 Technical Library, 9536 (electronic)
1 0123 Donna Chavez, 1011